

LA-UR-14-22435

Approved for public release; distribution is unlimited.

Title: DARHT Axis II Magnet Models

Author(s): Schulze, Martin E.

Intended for: Report

Issued: 2014-04-10



Disclaimer:

Los Alamos National Laboratory, an affirmative action/equal opportunity employer, is operated by the Los Alamos National Security, LLC for the National Nuclear Security Administration of the U.S. Department of Energy under contract DE-AC52-06NA25396. By approving this article, the publisher recognizes that the U.S. Government retains nonexclusive, royalty-free license to publish or reproduce the published form of this contribution, or to allow others to do so, for U.S. Government purposes. Los Alamos National Laboratory requests that the publisher identify this article as work performed under the auspices of the U.S. Department of Energy. Los Alamos National Laboratory strongly supports academic freedom and a researcher's right to publish; as an institution, however, the Laboratory does not endorse the viewpoint of a publication or guarantee its technical correctness.

DARHT Axis II Magnet Models

Introduction

There are known errors in the magnetic fields used to model the Axis II accelerator in the optics codes, XTR and LAMDA. These are due to the changes in the cell geometry and the proximity of the Metglas cores to the magnet coils. These were initially investigated by Houck [1] prior to the design change which resulted in adding 1.0 inch to the length of the accelerator cells. The interaction with the Metglas results in a shift and asymmetry in the magnetic field in addition to some field enhancement.

Magnet models for the DARHT Axis II accelerator magnets were developed prior to modifications of the cells to improve the voltage standoff. New models have been developed representing the present cell configuration. The original and extended intercell magnets have also been modeled in the presence of nearby cells. Prior models did not consider the effect of the Metglas in the nearby cells for the extended intercell magnets. The resulting magnet models differ slightly from the original models.

All magnet models were made on the basis of the nominal accelerator cell layout. The actual positions of each cell will vary from this nominal position. In addition, there is evidence that every time maintenance (cell cleaning and/or replacement) is performed on the accelerator, the location and alignment of the accelerator solenoids will shift.

Bucking Coil, Anode 1 and Anode 2

These magnet models are not significantly affected by nearby Metglas and existing magnet models need not be changed. The magnet model for the bucking coil, anode 1 and anode 2 magnets shows excellent agreement with measurements of the new bucking coil.

Anode 3

The effect of the nearby Metglas cores in the injector cells will distort the anode 3 magnetic field. The dimensions of the anode 3 solenoid coil are taken from the mechanical drawings and agree with Ref. [1] dimensions.

A study of the existing information for the anode 3 solenoid reveals many discrepancies relating to the actual number of turns, orientation relative to injector cells and the magnet model used in the optics codes.

1. Appendix E of reference [1] states that a comparison of magnetic measurements made at SLAC (without Metglas and a POISSON simulation was used to set the number of turns at 618. New POISSON simulations show that to achieve a peak field of 7.95 G/A (see Figure 2) without Metglas requires about 636 turns. This is a 3% discrepancy.
2. The SLAC measurements and subsequent measurements made of anode 3 in situ with the injector cell block shown in Figures 1 and 2 (Anode#3 (H2 10/18/01)) show an asymmetry and enhancement of the anode 3 field. There is very good agreement between a POISSON simulation and measurements in the presence of the injector cells as shown in Figure 1. However, in the POISSON simulation from Ref. [1], 582.7 turns were used. This is significantly

different from the value of 618 quoted above from the same reference. An independent POISSON calculation using this model from Ref. [1] and comparison with the data and the old XTR fit shows similar agreement as shown in Figure 3.

3. An examination of this POISSON input file shows that the dimensions of the Metglas are wrong. The inner radius of the Metglas is about 3" larger than the actual configuration and this has a significant effect on the field distribution. The agreement between the incorrect POISSON model (Metglas geometry and number of turns) and the data cannot be explained. Figure 4 shows a comparison of a POISSON simulation with the correct magnet model, old XTR fit and the measurements. With the as built dimensions of the Metglas, the anode 3 field falls off more rapidly as one would expect.
4. The mechanical drawings for the inner (21G9446) and outer (24P3666) coils specify a minimum of 49 turns per layer with 12 layers or 588 turns in one place and a minimum of 50 turns per layer with 12 layers or 600 turns in another place on the same drawing. Examination of the magnet model suggests the possibility of a maximum of 55 turns per layer.

Due to the above discrepancies and errors, a new model of the anode 3 solenoid has been developed using POISSON. We assume 636 turns and a spacing of 53.721 cm between the center of the anode 3 solenoid and the first injector cell solenoid (per DWG 47Y1745300). The POISSON model includes the complete injector cell block with a cell spacing of 53.95 cm as shown in Figure 5. The nominal cell-to-cell spacing is 53.9496 cm and we use 53.95 cm in the POISSON simulations. The old spacing was 51.406 cm. Figure 6 shows the POISSON model with the new and old XTR fits. The new simulation and fit is very close to the old fit and should not significantly affect the optics simulation. The parameters for the XTR fit are given in Appendix 1. Modeling of the Metglas cores used the nominal dimensions of the cores and assumed 1010 low carbon steel with a 75% fill factor. As pointed out in Ref. [1], the Metglas cores are far from saturation and no non-linear effects are observed.

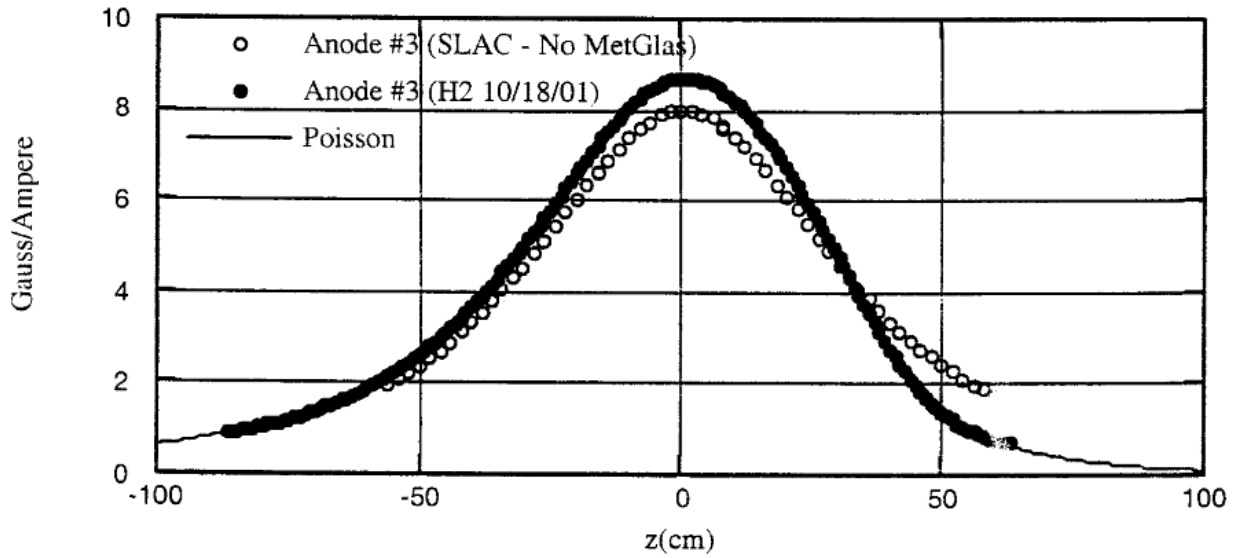


Figure 1: Figure 4 of Ref. [1] showing measurements of the anode 3 solenoid with and without the Metglas from Cell Block 1 including a POISSON simulation

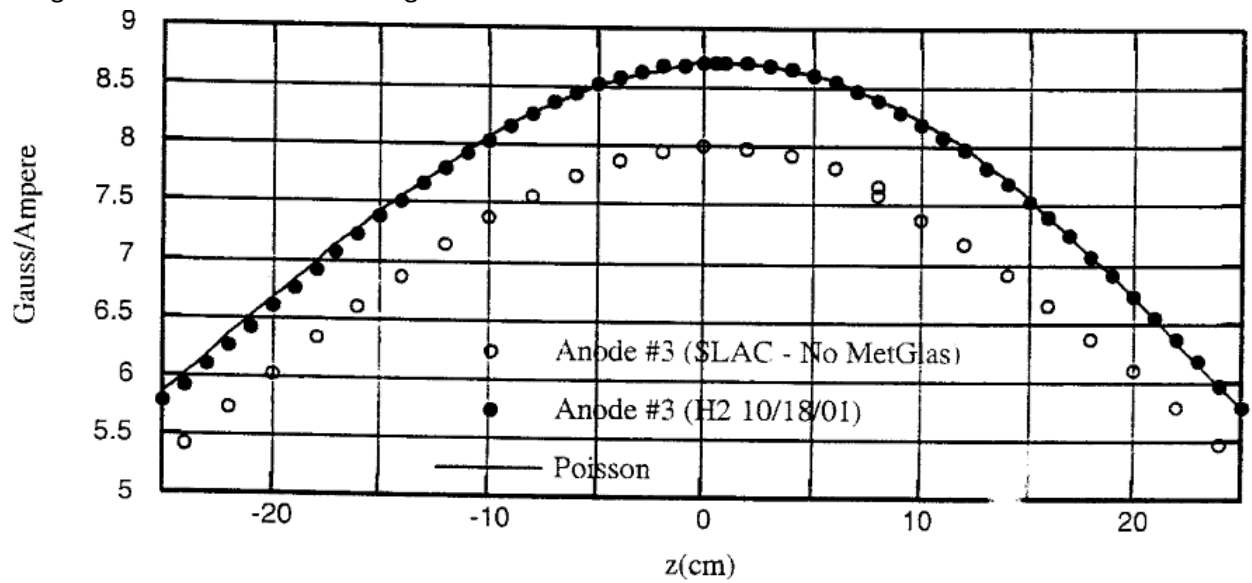


Figure 2: An expanded view of Figure 4 from Ref. [1] showing the fields in the central region of the magnet.

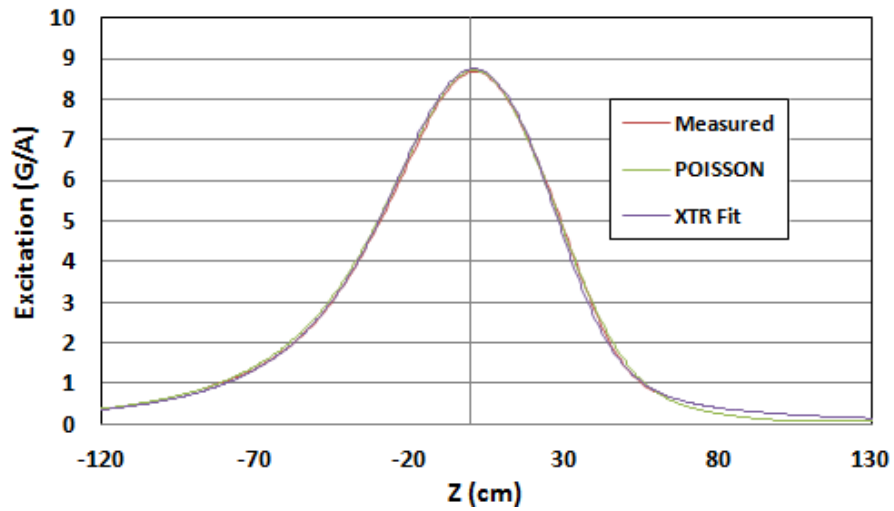


Figure 3: Measurement and simulation (POISSON) of Anode 3 solenoid in presence of CB1.

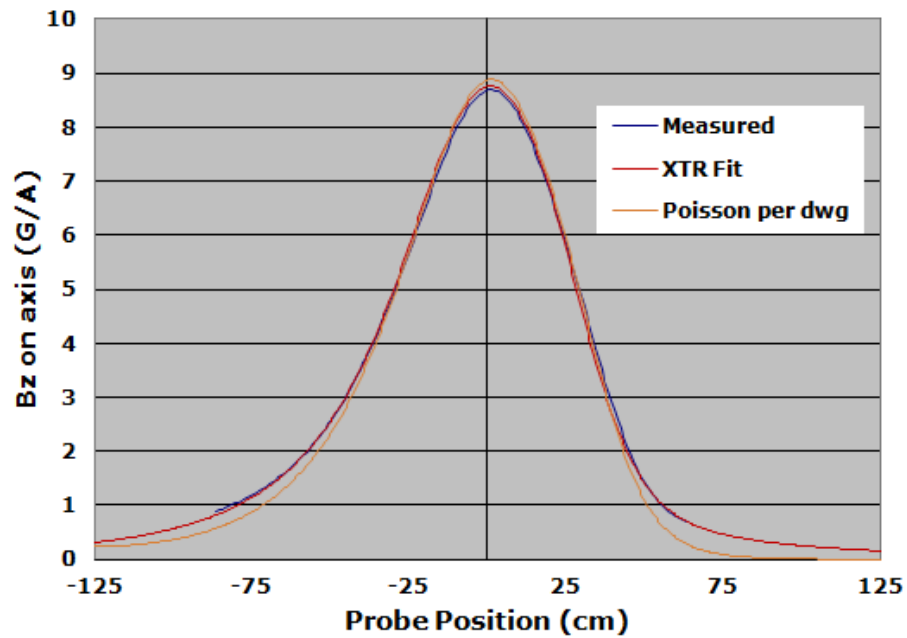


Figure 4: Anode 3 solenoid with correct orientation and dimensions of injector solenoids compared to “measured” and old XTR fit

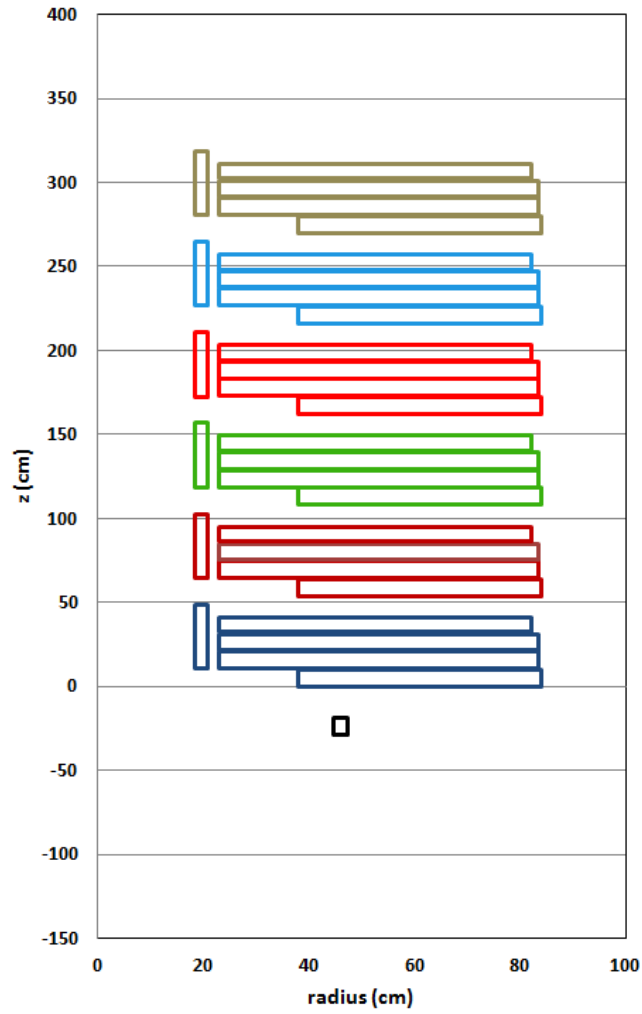


Figure 5: POISSON model of anode 3 and injector cell block.

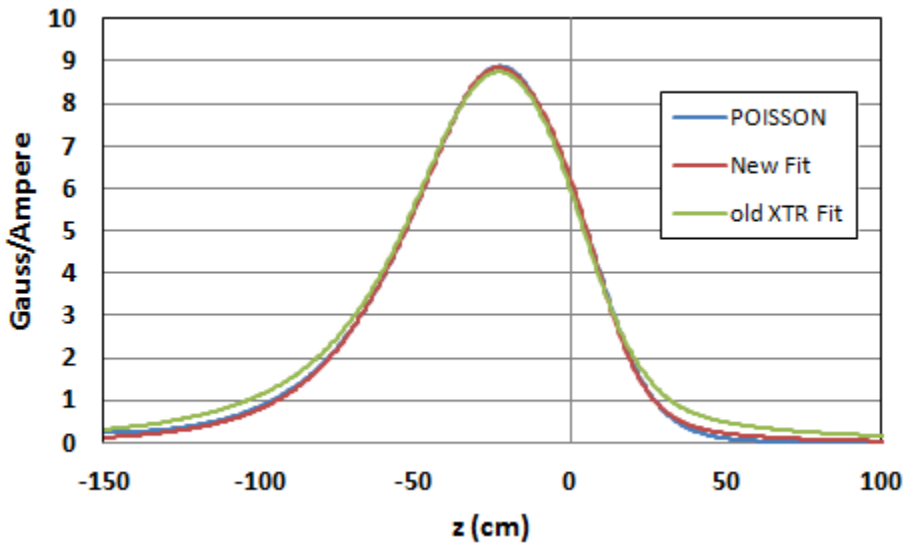


Figure 6: POISSON simulation of anode 3 with net and old XTR fits.

Injector Cell Solenoids

The layout of the injector cell solenoids relative to the Metglas is shown in Figure 7. Using the POISSON model described above, each injector cell solenoid is turned on and the magnet model is determined from the POISSON simulation. Injector cell solenoids 1 and 6 were fit using two magnet models to account for the asymmetry in the field distribution. The POISSON model used the actual number of turns for all magnets. Unique fits to each of the injector cell solenoids have been determined taking into account the number of turns in each magnet. The fits are given in Appendix A. Cell solenoid 6 exhibits a resistance indicating one shorted layer as described in Appendix B. This is reflected in the XTR fit in Appendix A.

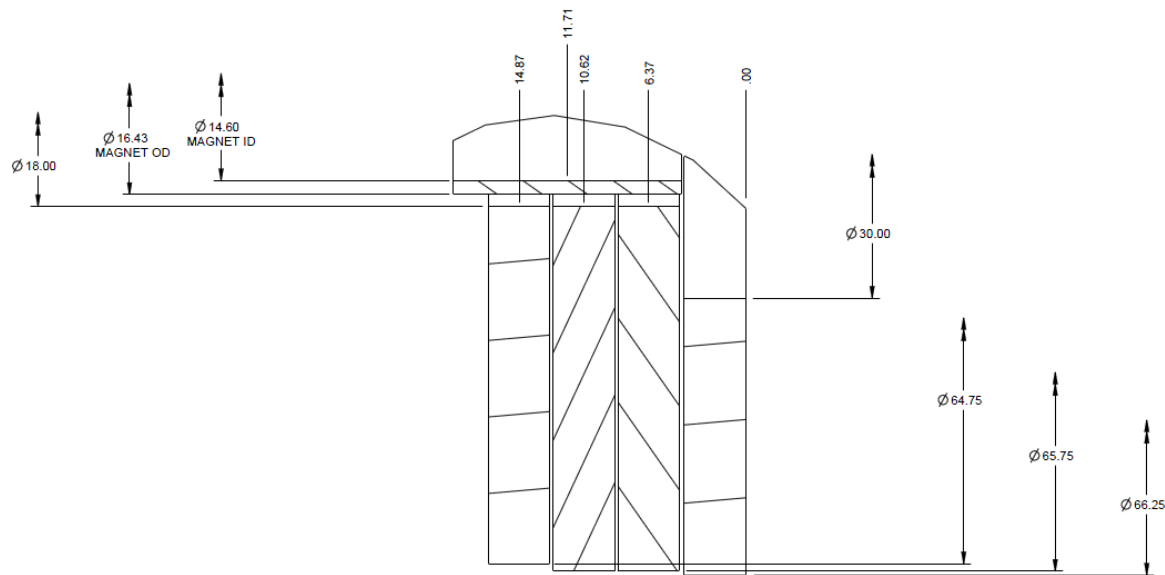


Figure 7: DARHT Injector cell Metglas dimensions with solenoid.

Accelerator Cell Solenoids

There is an average of 2332 turns in the original accelerator cell solenoids with a standard deviation of 1%. The six new NETC solenoids have an average of 2360 turns. The four interior cells in each cell block (six for cell block 2) are essentially identical based on the POISSON simulation. The magnet and cell locations for the POISSON model for cell block 2 are shown in Figure 8. Also shown in Figure 8 are the standard intercell and the extended intercell configurations. The first and last cells have small differences from the interior cells. The fields for these solenoids are only slightly influenced by the type of nearby intercell or lack thereof. The configuration without an intercell magnet was not modeled because there is only a 0.25" length difference compared to the standard intercell configuration. The POISSON models for the different entrance cell configurations are presented in Figure 9. The POISSON models for the different exit cell configurations are presented in Figure 10. Figure 11 compares the POISSON simulations of the entrance and exit cell solenoids. The beginning and ending cell solenoids are each fit with two XTR solenoid distributions. All interior cells are fit with a single XTR solenoid

distribution. The distributions are presented in Appendix A. Specific fits are provided for the degraded cells based on the note in Appendix B. The degraded accelerator cells are 21, 24, 26, 43, 72 and 73.

In the prior optics models of Axis II, the peak solenoid fields are about 0.2 cm upstream (towards the cathode) from the mechanical center of the respective solenoid for cells 1 through 5 (1 through 7 for cell block 2) and the peak solenoid field for the last (exit) cell is about 0.7 cm upstream (towards the cathode) from the mechanical center of the respective solenoid. As a result the location of the solenoid field was shifted from its physical location. This is reflected in Figure 1 of Appendix C.

The new POISSON models show that the location of the peak field corresponds with the physical location for all interior cell solenoids in a cell block. The locations of the entrance and exit cell solenoid fields are shifted as presented in Appendix A.

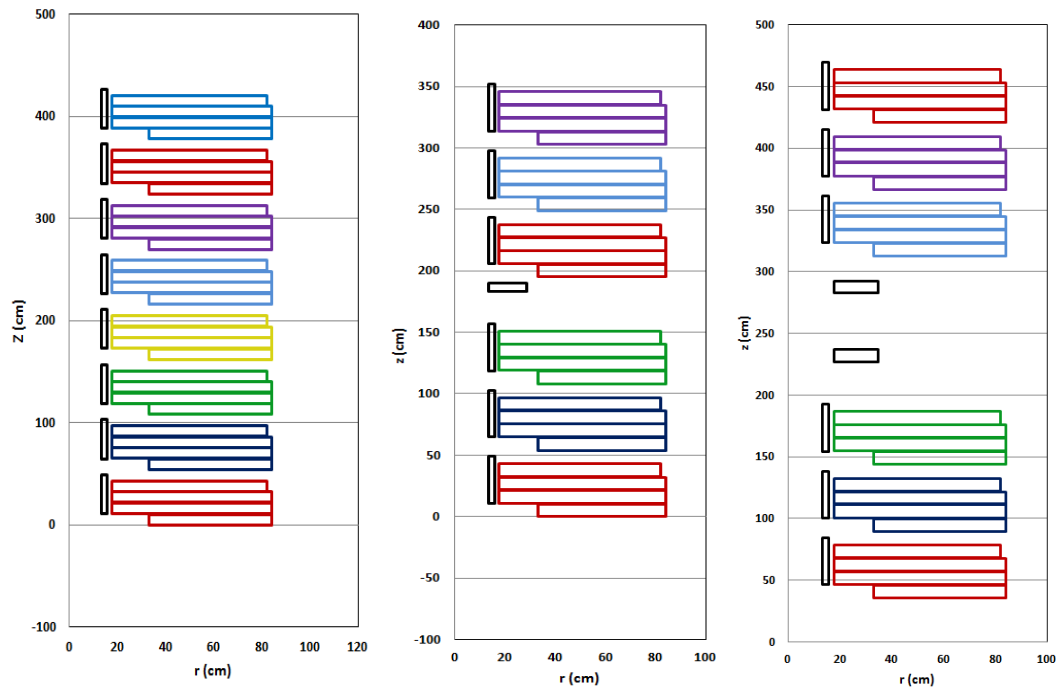


Figure 8: Poisson model for cell block 2 is on left. Poisson model for intercell solenoid is in middle. Poisson model for extended intercell solenoids is on right. The Metglas cores for each cell are shown in a different color and the solenoid coils are shown in black. The beam direction is in positive z direction.

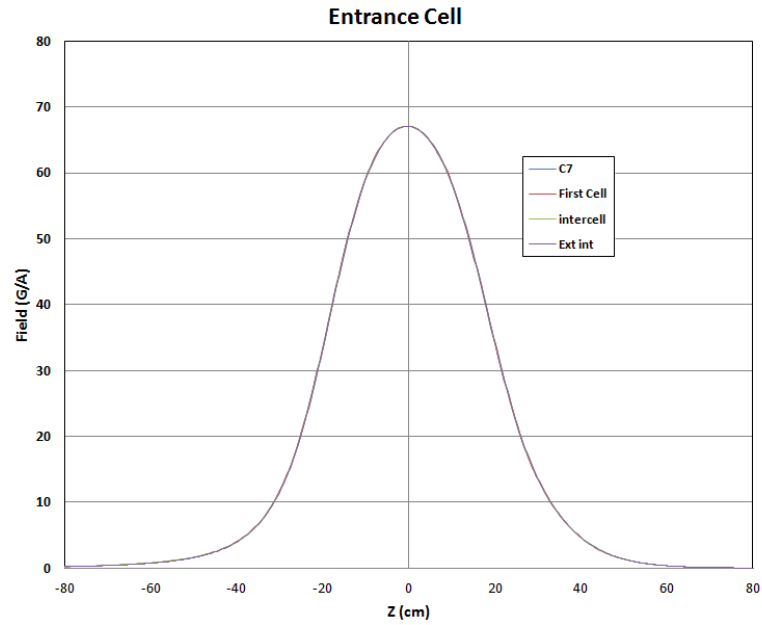


Figure 9: Comparison of POISSON simulations of the axial magnetic field in the different types of entrance cells for the accelerator.

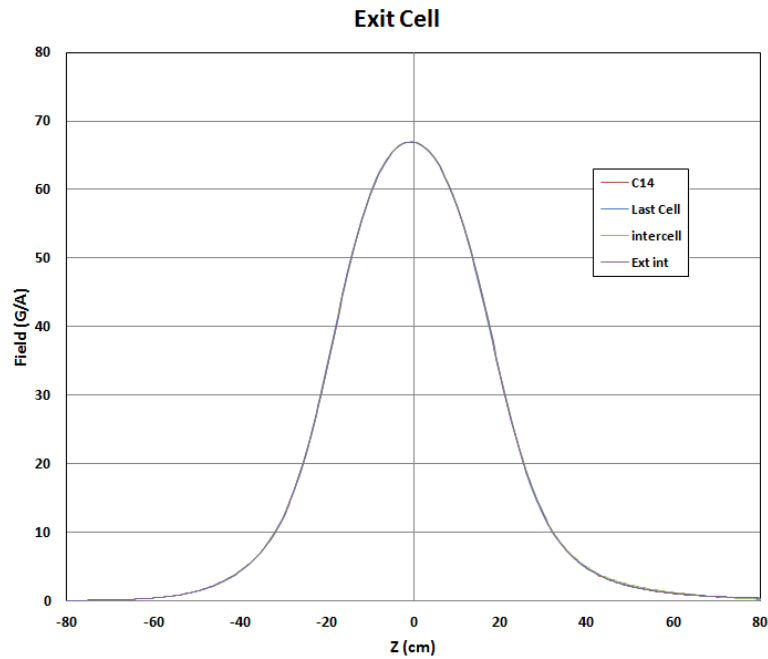


Figure 9: Comparison of POISSON simulations of the axial magnetic field in the different types of exit cells for the accelerator.

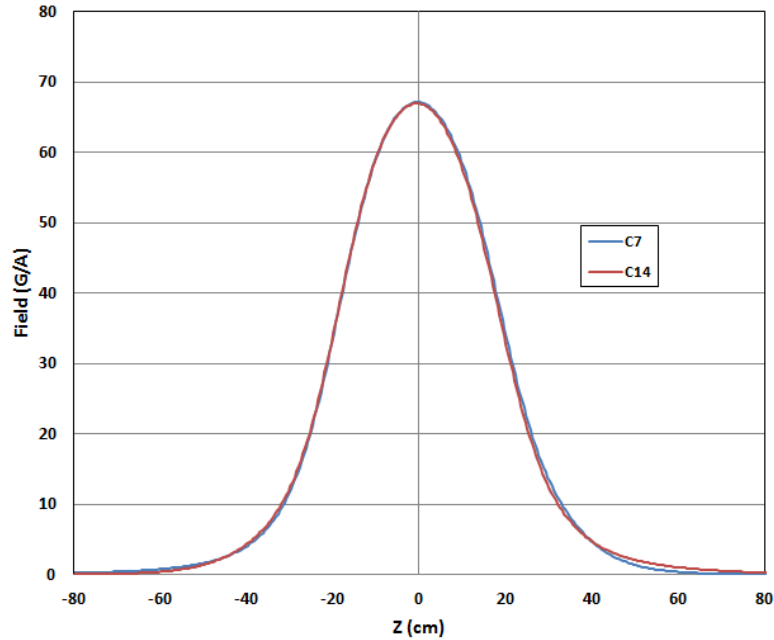


Figure 11: Comparison of axial field for the entrance and exit cell solenoids for cell block 2.

Intercell Solenoids

There are two types of intercells on the DARHT Axis II accelerator. They are identified as intercell and extended intercell. The intercell solenoids were modeled using the configuration on the middle layout in Figure 8. The extended intercell solenoids were modeled using the configuration on the RHS of Figure 8. The intercell solenoid was fit using two XTR models to account for the asymmetry as presented in Appendix A. Each of the extended intercell solenoids was also fit with two XTR models as given in Appendix A. The fits to the extended intercell solenoids are close to mirror images as shown in Figure 12.

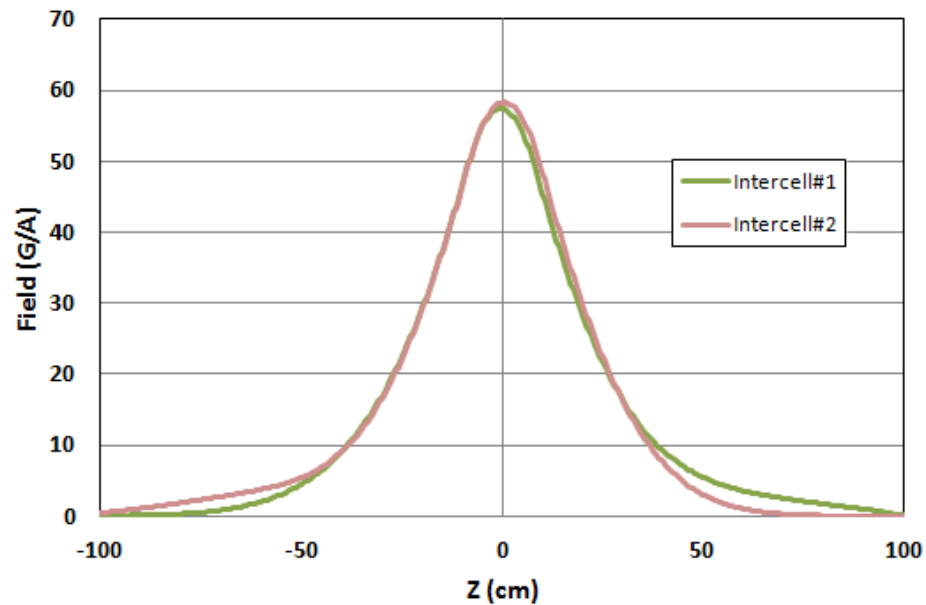


Figure 12: Axial fields for extended intercell solenoids

Summary

Magnet models for all accelerator magnets that are impacted by the refurbished accelerator cells have been developed and are presented in Appendix A. Some of the existing accelerator cells have reduced excitation functions due to shorted layers as described in Appendix B. Magnet models for these degraded solenoids are given in Appendix A. Appendix C describes an effort to determine the more precisely the locations of the magnets in Axis II. Significant differences between the optics models and as built configuration were identified. All of the results of this report have been used to more accurately define the accelerator configuration and magnet models for developing new optics tunes for the DARHT Axis II accelerator.

[1] DARHT Tech Note 257

APPENDIX A

New XTR Fits for Axis II Magnets

Magnet	Name	L_{eff} (cm)	a_{eff} (cm)	B (G/A)	n	α	Z_{offset} (cm)	Turns
Anode 3	anode31n	23.2	39.08	4.97	1.863	.000061	-18.25	636
	Anode32n	18.6	35	5.78	3.75	.000765	10.45	
Injector C1	injcimag12n	42.4	20.45	2.01	0.1	.0048	29.12	2333
	injcimag11n	37.3	19.9	59.68	2.13	.000195	-0.155	
Injector C2	injcimag2	39.25	21.7	59.7	2.13	.000272	0.1	2335
Injector C3	injcimag3	39.34	21.7	58.79	2.13	.000273	0.1	2299
Injector C4	injcimag4	39.4	21.7	59.1	2.13	.000272	0.1	2313
Injector C5	injcimag5	39.4	21.7	59.11	2.13	.000272	0.1	2314
Injector C6	injcimag61	39	19.35	53.68	2.14	.000205	-0.53	2329
	injcimag62	27	28	1.238	1.9	.0001	42.16	
Starting cell 7,15,27, etc	Cmagi2	42	19	2.2	1.35	.0036	24.5	2332
	Cmagi1	40	16.3	67.3	1.65	.000565	-0.29	
Cell 21	cmagi212	42	19	1.83	1.35	.0036	24.5	
	cmagi211	40	16.3	56.13	1.65	.000565	-0.29	
Middle Cell	cmagnew	40.2	16.2	67.35	1.67	.000476	0	2332
Cell24	Cmag24	40.2	16.2	61.74	1.67	.000476	0	
Cell43	Cmag43	40.2	16.2	56.13	1.67	.000476	0	
Cell72	Cmag72	40.2	16.2	61.74	1.67	.000476	0	
Cell73	Cmag73	40.2	16.2	56.13	1.67	.000476	0	
Cell26	Cmago262	43	25	0.917	1.2	.001	32	2332
	Cmago261	40.1	15.95	61.46	1.59	.00055	-0.38	
Intercell	intcmag1n	26	20	7.4	1	.00228	-30	2511
	intcmag2n	3.2	28.3	82.1	1.85	.00108	0.288	
Extended intercell #1	nuintmag12	60.2	5.12	1.73	4	.00125	67.3	
	nuintmag11	18.2	48.4	57.39	1.067	.00054	-0.33	
End Cell 14, 20, etc	cmago2	43	25	1	1.2	.001	32	2332
	cmago1	40.1	15.95	67.05	1.59	.00055	-0.38	
Extended intercell #2	nuintmag21	19.7	94	58.27	0.85	.00087	0.47	
	nuintmag22	90	6	2.85	3.3	.00094	-58.0	

APPENDIX B

Cell Solenoids – Degradation Estimate

It is well known and documented that there are some cell solenoids that exhibit shorted turns. Attempts have been made to determine the number of shorted turns in magnets that have resistances that are significantly lower than nominal. The initial method was based on the average and standard deviation in the resistance of the “good” cell solenoids. The ratio of the resistance in a “bad” solenoid to this average is the degradation. This degradation represents the percentage of turns that are not shorted.

Note that a much more accurate determination could be made using the original travelers for each solenoid.

The injector cells show two questionable solenoids (4 and 6). Solenoid 4 is probably not degraded but solenoid 6 is definitely low. The average resistance and standard deviation for solenoids 1, 2, 3 and 5 is 16.27 and 0.23 Ohms respectively.

The average resistance and standard deviation for the accelerator solenoids is 12.275 and 0.286 Ohms respectively. This was determined by not including solenoids with too high a resistance (30, 33 and 53) and too low a resistance (21, 24, 26, 43, 67 and 73).

Recent analysis of the thermal stresses by W. Tuzek has shown excessive thermal stresses at the end of the solenoid coil indicating that turn-to-turn shorts are likely to occur at the magnet ends. This implies that complete layers will be shorted. Analysis of magnetic measurements of the degraded bucking coil shows that the field is almost exactly 2/3 of the new bucking coil. This is again consistent with 2 of the 6 layers being shorted. As a result, we assume that an integral number of layers has shorted and determine the new excitation function on this basis rather than the ratio of the new and old resistances. The table below strongly supports this approach. Since there are 12 layers in each coil, one shorted layer would result in a degradation of 91.67, while two shorted turns would give a degradation of 83.33. These numbers are extremely close to the degradation determined by the change in resistance.

Magnet	Resistance (Ohm)	Comment	Degradation by resistance	Degradation from shorted turns
Anode2	1.841	Resistance consistent with 3 shorted layers	43.7	50
4	15.737	Resistance is $\sim 2.3 \sigma$ lower than average of cells 1, 2, 3 and 5. The need to correct for this solenoid is questionable.	100	100
6	15.024	Resistance is $\sim 5.4 \sigma$ lower than average of cells 1, 2, 3 and 5.	92.3	91.67

21	10.336	Resistance is ~6.8 σ lower than average.	84.2	83.33
24	11.156	Resistance is ~3.9 σ lower than average Observed degradation on 6/18/08	90.9	91.67
26	11.301	Resistance is ~3.4 σ lower than average Resistance has always been low since 2006	92.1	91.67
43	10.247	Resistance is ~7.1 σ lower than average	83.5	83.33
72	11.26	Resistance consistent with 1 shorted layer	90.3	91.67
73	9.949	Resistance is ~8.1 σ lower than average	81.1	83.33

APPENDIX C

Magnet Location Errors in the Axis II Accelerator

There are known errors in the magnetic fields used to model the Axis II accelerator in the optics codes, XTR and LAMDA. These are due to the changes in the cell geometry and the proximity of the Metglas cores to the magnet coils. These were initially investigated by Houck [1] prior to the design change which resulted in adding 1.0 inches to the length of the accelerator cells. The interaction with the Metglas results in a shift and asymmetry in the magnetic field in addition to some field enhancement. An effort is underway to develop new magnet models for all accelerator magnets. In order to obtain accurate models, the locations of the magnets and cells must be known. The magnet locations presently used in the optics codes are from an analysis by Smith [2]. Smith's analysis is based on information in Ref. [1] and DWG 47Y640500 and laser tracker data for specific magnets based on measurements made in 2009. Since 2009, the accelerator has been disassembled and assembled many times for cell cleaning and replacement. The mechanical design team provided DWG 47Y1745300 on 1-13-14 as their baseline database of the as built locations of the magnets. DWGs 47Y640500 and DWG 47Y1745300 are essentially identical after correcting for the new cathode location. A comparison of DWG 47Y1745300 and the XTR magnet locations identified significant differences in the magnet locations especially in the injector, injector cells, extended intercells and the last cell magnet of each cell block. Figure 1 shows the position offset between XTR and DWG 47Y1745300. The systematic offset on the cells in each accelerator cell block is based on old data suggesting the magnetic center of each solenoid is offset by 2 mm with the exception of the last solenoid in each cell block is offset by 7 mm.

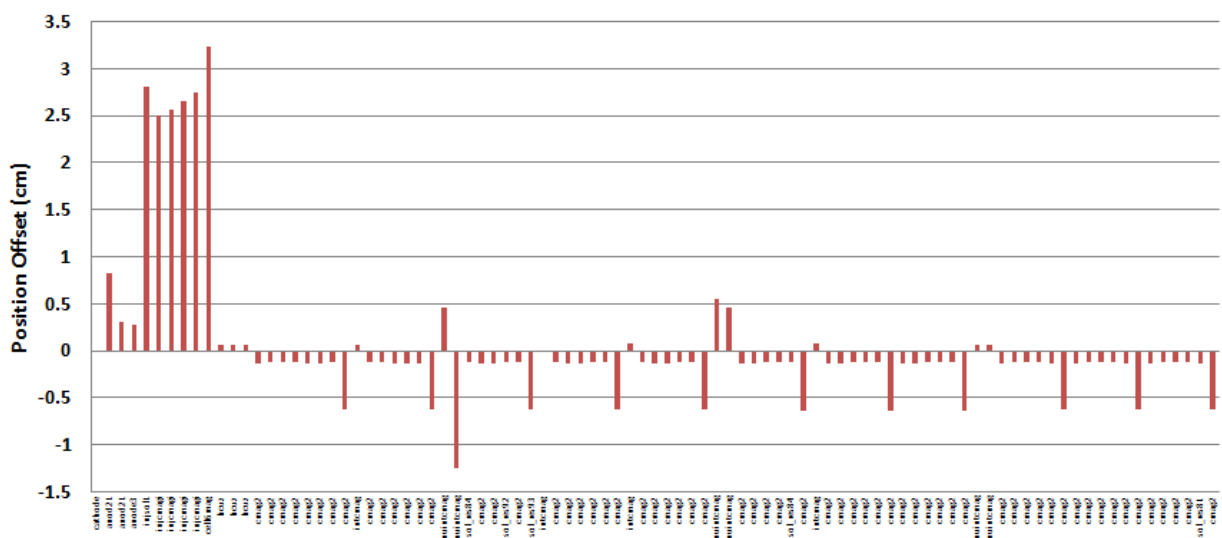


Figure 1: Position offset for Axis II magnets (difference between XTR/LAMDA and DWG 47Y1745300)

As a result of the discrepancies in Figure 1, especially in the injector cells, Measurements were made for most magnets through cell 21 on 1-23-14. The “old” intercell magnets and the anode magnets were not

measured. The results are shown in Figure 2. All measurements are made with respect to the location of cell solenoid 7 on DWG 47Y174530. The results indicate the following:

1. The XTR/LAMDA locations for the injector cell solenoids are all off by about 3 cm each
2. The BCUZ2 and BCUZ3 solenoids are significantly different from the XTR/LAMDA and “as built” configurations
3. The extended intercell solenoids are significantly different from the XTR/LAMDA and “as built” configurations

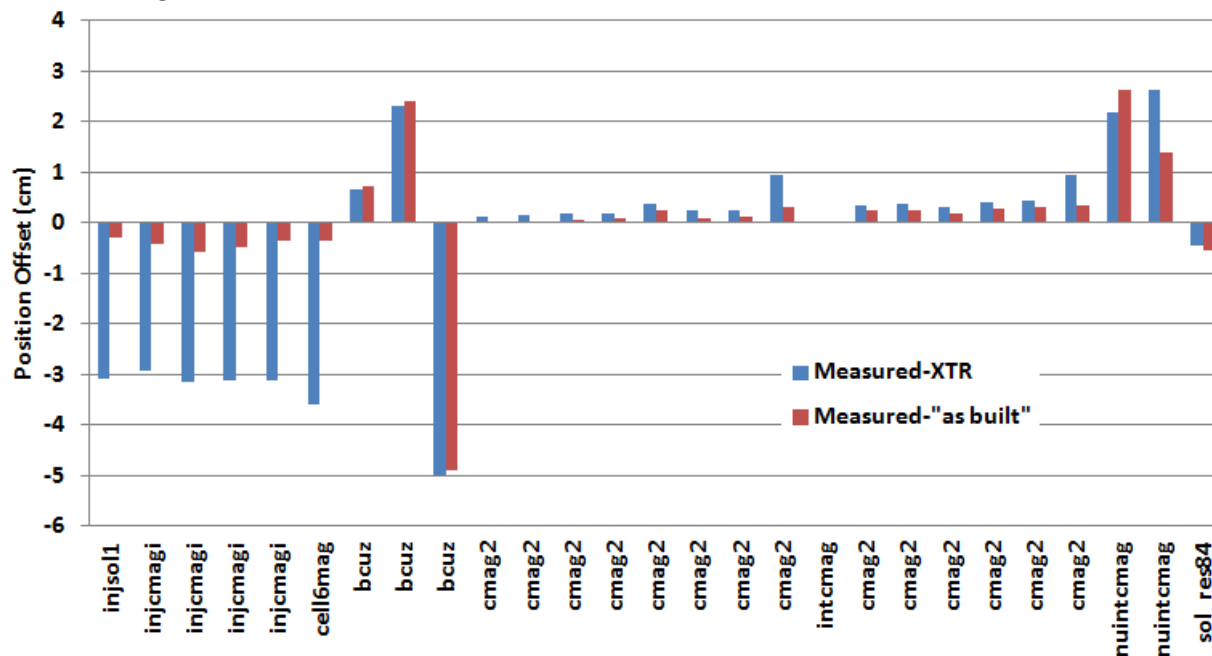


Figure 2: Comparison of measured magnet positions and XTR and “as built” configurations through cell 21

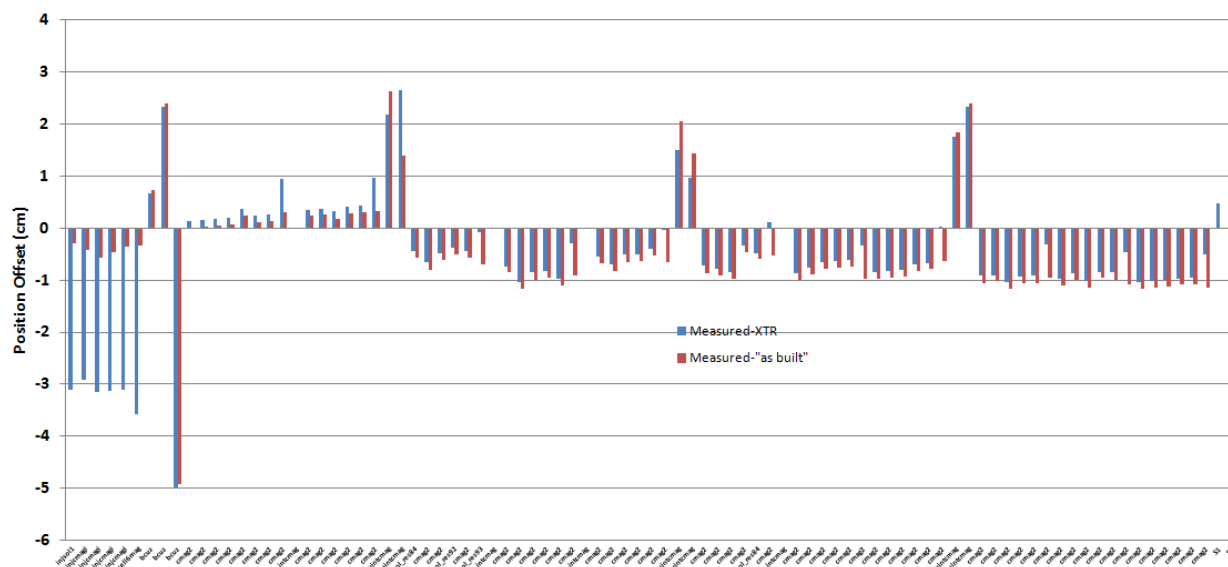


Figure 3: Comparison of measured magnet positions and XTR and “as built” configurations through cell 21

The entire machine (except for the anode and “old” intercell magnets) up through the S2 solenoid was measured on 1-27-14. The results are shown in Figure 3. The same discrepancies are found.

[1] DARHT Tech Note 257

[2] DARHT Tech Notes 287, 270 and 272